Journal of
Astronomical Telescopes,
Instruments, and Systems

AstronomicalTelescopes.SPIEDigitalLibrary.org

Microwave SQUID multiplexing for the Lynx x-ray microcalorimeter

Douglas A. Bennett
John A. B Mates
Simon R. Bandler
Daniel T. Becker
Joseph W. Fowler
Johnathon D. Gard
Gene C. Hilton
Kent D. Irwin
Kelsey M. Morgan
Carl D. Reintsema
Kazuhiro Sakai
Daniel R. Schmidt
Stephen J. Smith
Daniel S. Swetz
Joel N. Ullom
Leila R. Vale
Abigail L. Wessels

Douglas A. Bennett, John A. B Mates, Simon R. Bandler, Daniel T. Becker, Joseph W. Fowler, Johnathon D. Gard, Gene C. Hilton, Kent D. Irwin, Kelsey M. Morgan, Carl D. Reintsema, Kazuhiro Sakai, Daniel R. Schmidt, Stephen J. Smith, Daniel S. Swetz, Joel N. Ullom, Leila R. Vale, Abigail L. Wessels, "Microwave SQUID multiplexing for the Lynx x-ray microcalorimeter," *J. Astron. Telesc. Instrum. Syst.* **5**(2), 021007 (2019), doi: 10.1117/1.JATIS.5.2.021007.

Downloaded From: https://www.spiedigitallibrary.org/journals/Journal-of-Astronomical-Telescopes,-Instruments,-and-Systems on 25 Apr 2019
Terms of Use: https://www.spiedigitallibrary.org/terms-of-use

Microwave SQUID multiplexing for the Lynx x-ray microcalorimeter

Douglas A. Bennett,[a,*] John A. B Mates,[b] Simon R. Bandler,[c] Daniel T. Becker,[b] Joseph W. Fowler,[a,b] Johnathon D. Gard,[b] Gene C. Hilton,[a] Kent D. Irwin,[d] Kelsey M. Morgan,[a,b] Carl D. Reintsema,[a] Kazuhiro Sakai,[c,e] Daniel R. Schmidt,[a] Stephen J. Smith,[c,e] Daniel S. Swetz,[a] Joel N. Ullom,[a,b] Leila R. Vale,[a] and Abigail L. Wessels[b]
[a]National Institute of Standards and Technology, Boulder, Colorado, United States
[b]University of Colorado at Boulder, Boulder, Colorado, United States
[c]NASA—Goddard Space Flight Center, Greenbelt, Maryland, United States
[d]Stanford University, Department of Physics, Palo Alto, California, United States
[e]CRESST and University of Maryland, Baltimore County, Maryland, United States

Abstract. The Lynx x-ray microcalorimeter (LXM) is an imaging spectrometer for the Lynx satellite mission, an x-ray telescope being considered by NASA to be a new flagship mission. Lynx will enable unique astrophysical observations into the x-ray universe due to its high angular resolution and large field of view. The LXM consists of an array of over 100,000 pixels and poses a significant technological challenge to achieve the high degree of multiplexing required to read out these sensors. We discuss the details of microwave superconducting quantum interference device (SQUID) multiplexing and describe why it is ideally suited to the needs of the LXM. This case is made by summarizing the current and predicted performance of microwave SQUID multiplexing and describing the steps needed to optimize designs for all the LXM arrays. Finally, we describe our plan to advance the technology readiness level (TRL) of microwave SQUID multiplexing of the LXM microcalorimeters to TRL-5 by 2024. © *The Authors. Published by SPIE under a Creative Commons Attribution 4.0 Unported License. Distribution or reproduction of this work in whole or in part requires full attribution of the original publication, including its DOI.* [DOI: 10.1117/1.JATIS.5.2.021007]

Keywords: multiplexing; superconducting resonators; microcalorimeters.

Paper 18098SS received Nov. 1, 2018; accepted for publication Mar. 7, 2019; published online Mar. 22, 2019.

1 Introduction

The Lynx x-ray microcalorimeter (LXM) is an imaging spectrometer proposed as part of the Lynx satellite mission concept currently under study to be a National Aeronautics and Space Administration (NASA) flagship mission.[1] Lynx will enable unique astrophysical observations into the x-ray universe due to its high angular resolution and large field of view. Because Lynx will improve sensitivity by two orders of magnitude compared to Chandra,[2] it will be able to penetrate into the epoch of reionization to detect x-rays from black holes lighting up the first galaxies and map the baryons in the Cosmic Web and galactic halos.[3] Since the majority of the baryonic matter in the universe is visible in either x-ray emission or absorption, Lynx will be a powerful tool for understanding the origins of the cosmos.

The LXM is one of three instruments proposed for the Lynx mission. The LXM consists of a cryogenic focal plane array with more than one hundred thousand pixels achieving spectral resolution better than 3 eV full width at half maximum (FWHM) at 0.2 to 7 keV.[4,5] It is a significant technological challenge to read out such a large array due to the high degree of multiplexing required. The LXM strategy to achieve this multiplexing factor is to use a combination of thermal[6] and electrical[7,8] multiplexing.

The proposed thermal multiplexing works by attaching multiple absorbers to each sensor through varying thermal conductances.[6] When a photon is absorbed, the pulse shape of the response is different for the different thermal conductances and can be used to identify which pixel absorbed the photon. When a sensor is used in this way for thermal multiplexing, it is called a hydra after the mythical, many-headed serpent.

The baseline for electrical multiplexing is microwave frequency multiplexing of superconducting quantum interference device (SQUID) amplifiers.[9–11] Microwave SQUID multiplexers (μMUX) transform the baseband signals from the detectors into frequency shifts of superconducting resonators at gigahertz frequencies, utilizing the large available bandwidth of microwave components to read out hundreds to thousands of sensors per coaxial cable. Over the last decade, there has been rapid progress in the development of microwave SQUID multiplexers to readout microcalorimeters.[12–16]

In this paper, we describe the theory of microwave SQUID multiplexing and show that it can meet the requirements of the LXM. This case is made by both reviewing the recent developments in microwave SQUID multiplexing and describing how microwave SQUID multiplexers will be optimized to meet the requirements of the sensors being considered for the LXM. Two types of microcalorimeters, transition-edge sensors (TESs) and metallic magnetic calorimeters (MMCs), are being considered for the LXM. This paper will focus on using microwave SQUID multiplexing to readout TESs. Microwave SQUID multiplexing is also the leading candidate to readout large arrays of MMCs[17,18] and the optimization described in this paper would also be useful for MMCs.[19]

*Address all correspondence to Douglas A. Bennett, E-mail: Douglas.Bennett@nist.gov

Downloaded From: https://www.spiedigitallibrary.org/journals/Journal-of-Astronomical-Telescopes,-Instruments,-and-Systems on 25 Apr 2019
Terms of Use: https://www.spiedigitallibrary.org/terms-of-use

2 Readout of the LXM Pixels

2.1 *Lynx X-Ray Microcalorimeter*

The LXM focal plane has been proposed to include a main array and two subarrays (Fig. 1).[1] The main array covers a 5 deg field-of-view with 1 in. pixels, with 3-eV energy resolution at 7 keV. In the central 1 deg of the main array, an enhanced main array provides finer imaging capability and improves energy resolution to 1.5 eV using 0.5 in. pixels. Adjacent to the main array, an ultra-hi-res array provides 0.3-eV energy resolution up to 0.75 keV, accepting a much greater x-ray flux than the main array. All told, fully populating the LXM focal plane requires 102,600 pixels. The burden to read out all of these pixels will be met using a combination of thermal and electrical multiplexing.

The thermal multiplexing is based on the hydra pixels described in detail elsewhere in these proceedings,[21] each consisting of a microcalorimeter that is coupled to multiple discrete absorbers by thermal links with different thermal conductances. Hydra detectors have been under development for over a decade by the NASA Goddard Space Flight Center (GSFC).[6] The links are varied so as to give a different characteristic pulse shape for x-ray photons absorbed in each of the absorbers. The rising edge of each pulse is used to determine in which pixel the photon was absorbed, and the energy of the pulse is determined using an optimal filter algorithm that is calibrated for each specific absorber element. NASA GSFC has demonstrated nine-absorber hydra TESs with <3 eV resolution at 6 keV and 20-absorber hydra TESs with 3.4 eV at 6 keV.[21]

Readout in a photon starved environment can be considerably simplified with hydra designs in which multiple spatial pixels are connected to a single detector and a single readout channel. A multiplexing circuit reading out hydra detectors must then be able to track the maximum slew rate of the fastest hydra pixel. The reduction in detector count and resonator count significantly eases both power dissipation and complexity, in both the cryogenic components and in the room-temperature electronics, and could be critically enabling for a satellite instrument like the LXM.

Even with 25-fold thermal multiplexing the main array will require ~3500 high-speed TES detectors. We expect each of these detectors to receive x-ray pulses at ~10 counts per second (cps) for the highest resolution x-ray events (40 cps for the medium resolution case where the record length for determining the energy is four times shorter and 150 cps for the lowest energy resolution x-ray events),[1] with slew rates as high as 1.5 A/s, which the readout must be able to track. The total count rates in the other subarrays are similarly demanding and will require large multiplexer bandwidth to read out. Electrical multiplexing factors of hundreds are therefore required, for a range of bandwidths per sensor from 0.86 to 6 MHz. Table 1 in Sec. 3.2 summarizes the requirements for the different subarrays, along with their microwave SQUID multiplexer solutions.

2.2 *Microcalorimeter Multiplexing Technologies*

In a multiplexer, the signals from different input channels are multiplied by a basis set of modulation functions and summed into a common output channel. The signals are then separated and decoded by inversion of this basis. The three most important sets of orthogonal basis functions used to date to multiplex TES detectors are low duty-cycle boxcar functions used in time-domain multiplexing (TDM), sinusoidal functions used in

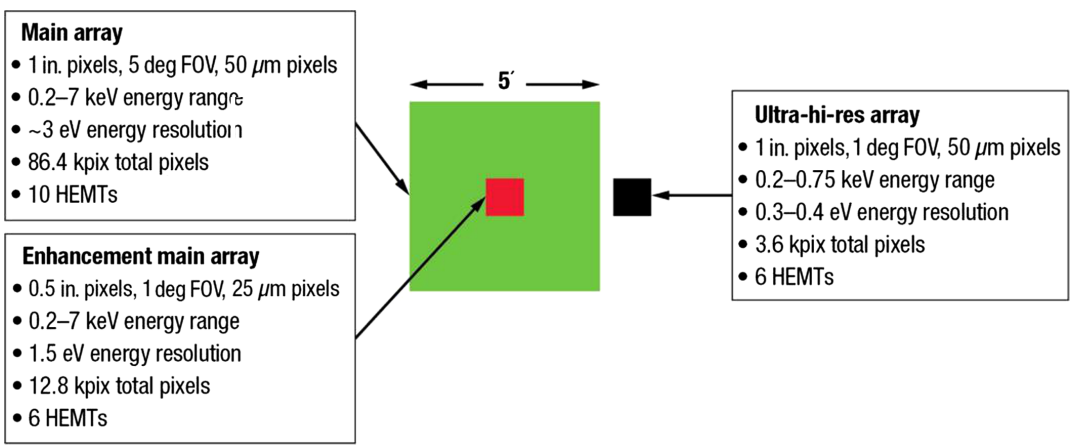

Fig. 1 Illustration of proposed LXM focal plane,[20] including detector and pixel requirements for the main array (green), the enhanced main array at its center (red), and the ultra-hi-res array next to it (black).

Table 1 Requirements for the various subarrays of the LXM. The ultra-hi-res array will not be read out at the same time as the main array and enhanced main array so at most 16 HEMTs will be operated at once.

	# of pixels	Hydra	Slew rate	Res. *BW*	Res./HEMT	# of HEMTs
Main array	86,400	5 × 5	1.5 A/s	1.4 MHz	400	10
Enhanced main array	14,400	5 × 5	6 A/s	5.6 MHz	100	6
Ultra-hi-res array	3600	n/a	0.85 A/s	0.86 MHz	667	6

Downloaded From: https://www.spiedigitallibrary.org/journals/Journal-of-Astronomical-Telescopes,-Instruments,-and-Systems on 25 Apr 2019
Terms of Use: https://www.spiedigitallibrary.org/terms-of-use

frequency-domain multiplexing (FDM), and Walsh functions used in code-division multiplexing (CDM).

The most technically mature multiplexing scheme for the readout of TES microcalorimeters is time-division multiplexing (TDM).[22,23] In TDM, the sensors are dc-biased and each is inductively coupled to its own first-stage SQUID that is modulated in time by a low duty-cycle boxcar function. Rows of SQUIDs are switched on sequentially in time, and columns of SQUIDs are read out in parallel. TDM readout enabled rapid scaling from single-pixel demonstrations in the early 1990s to multiple eight-column by 30-row (240-pixel) microcalorimeter arrays for x-ray spectroscopy today. However, in a TDM column with N sensors, each sensor's SQUID signal is sampled for only $1/N$ of the time, so high-frequency SQUID noise is aliased into the signal band, a problem that grows as $\sqrt{N}$.[22] Up to $N \approx 30$, this "multiplexing disadvantage" is almost negligible but it becomes significant for higher multiplexing factors. The readout noise referenced to the input of the multiplexer channel can be improved by increasing the coupling between the input coil and SQUID, but this decreases the maximum slew rate that can be achieved by the same factor.[7] Therefore, there is a trade-off between multiplexing factor, input referred readout noise, and maximum measurable slew rate. Furthermore, the state-of-the-art TDM has only achieved a total bandwidth of ~10 MHz per column, preventing the readout of large numbers of truly fast sensors.[23]

An alternative multiplexing scheme is MHz-band frequency-division multiplexing (FDM).[24] In FDM, the sensors are placed in series LC resonant circuits and ac-biased at different frequencies in a 1- to 5-MHz band. So far, FDM of microcalorimeters has produced a 6-pixel demonstration with an average resolution of ~3 eV at 6 keV.[25] FDM of bolometric sensors has achieved multiplexing factors of up to 176 detectors per line,[26,27] but the ~10 MHz total bandwidth again limits its usefulness for fast sensors.

CDM uses a different set of orthogonal modulation functions: Walsh codes, in which during each time step the signals from all dc-biased TESs are summed with equal weight but different polarity patterns.[28] In Φ-CDM,[29] the current signals from N microcalorimeters are passively summed in N different SQUIDs with different coupling polarities. A 32-channel Φ-CDM circuit with an array of TES x-ray microcalorimeters has been demonstrated giving single pixel energy resolutions from 2.4 to 3.0 eV FWHM, and obtained an energy resolution of the coadded spectrum of 2.77 eV at MnKα (5.9 keV).[30] While CDM eliminates the aliasing penalty of TDM, it does not ease the 10 MHz bandwidth limit.

For non-hydra x-ray microcalorimeters, all three techniques can provide a path to arrays of 10^3 pixels, and all three techniques are under consideration for the ATHENA x-ray integral field unit, an ~3000-pixel array scheduled to launch in 2031. However, due to the scale of the LXM array (~100,000 pixels) and the slew rates of the hydra microcalorimeters, more readout bandwidth is needed than existing TDM, CDM, or FDM techniques can reasonably provide. To perform the electrical multiplexing required for the LXM, a higher bandwidth multiplexing technique is required. As will be shown in the following sections, microwave SQUID multiplexing is capable of providing the necessary bandwidth.

2.3 *Principles of Microwave SQUID Multiplexing*

Microwave multiplexing dramatically increases the available bandwidth by moving the FDM carrier signals into the gigahertz regime. The microwave SQUID multiplexer (μMUX)[10,11] divides the bandwidth available in a high electron-mobility transistor (HEMT) amplifier among input channels of superconducting microwave resonators coupled to a common feedline, in a similar approach to that of microwave kinetic inductance detectors (MKIDs).[31]

A microwave SQUID multiplexer uses rf-SQUIDs inductively coupled to cryogenic sensors to modulate the frequency of microwave resonators (Fig. 2). By coupling these resonators to a common microwave feedline with each resonator designed to resonate at a different frequency, we can read out all the sensors simultaneously. A microwave tone placed on one resonance measures its frequency shift and thus its detector signal; a superposition of microwave tones, one for each resonator, measures all detectors at once.

This technique allows a dramatic increase in multiplexing factor. Balancing noise, cost, and availability of components, we have chosen to work with commercial HEMTs in the 4- to 8-GHz band. With high-Q (narrow-band) superconducting resonators and accurate frequency placement, we can fill this HEMT bandwidth with thousands of nonoverlapping resonances, each with its own SQUID. By digitally synthesizing the superposition of probe tones, we can read out all the SQUIDs simultaneously.

Flux-ramp modulation is applied to the rf-SQUIDs, in order to linearize the SQUID response.[32] By ramping the flux in the rf-SQUID at a fixed frequency (f_r) by a integer number of flux quanta (N), the resonant frequency of the resonator is modulated at a frequency of Nf_r. The flux in the SQUID can be determined by the relative phase shift of the modulated signal averaged over

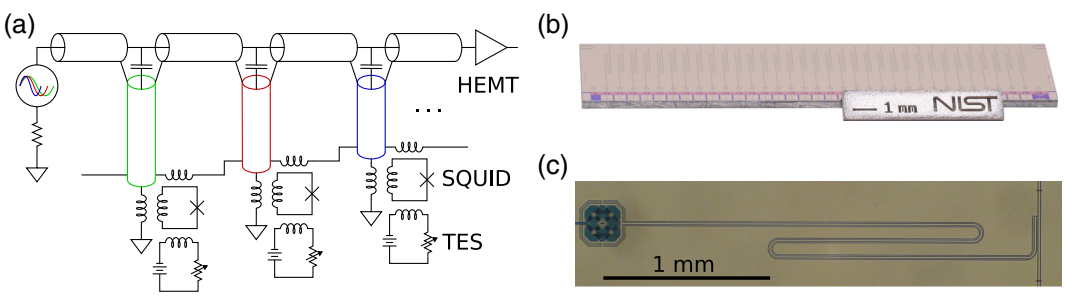

Fig. 2 (a) A schematic representation showing just three channels of a microwave SQUID multiplexing circuit with TESs. (b) A photograph of a 33-channel μMUX chip. (c) A close-up photograph showing a quarter-wave microwave resonator capacitively coupled to a feedline (right) and terminated with an rf-SQUID (left).

Downloaded From: https://www.spiedigitallibrary.org/journals/Journal-of-Astronomical-Telescopes,-Instruments,-and-Systems on 25 Apr 2019
Terms of Use: https://www.spiedigitallibrary.org/terms-of-use

the period of the flux-ramp. The flux-ramp is applied to the rf-SQUIDs in the multiplexer using a common set of wires to keep the wire count low. The limits that flux-ramp modulation place on the maximum measurable slew rate of the sensor and how this affects the bandwidth of the resonators will be described in Sec. 3.1. In the standard algorithm for flux-ramp demodulation, a single phase shift is determined for each period of the flux ramp signal. Therefore, the current through the sensor is measured at a sampling rate equal to the flux-ramp frequency.

2.4 *Microwave SQUID Multiplexing Demonstrations*

To evaluate the suitability of microwave SQUID multiplexing to readout the LXM, we should review the relevant demonstrations. The first demonstration of microwave SQUID multiplexing of TES microcalorimeters on scales larger than a few pixels is from the pathfinder project, SLEDGEHAMMER. This instrument uses 300-kHz resonator-bandwidth microwave SQUID multiplexer designs. SLEDGEHAMMER is a prototype high-resolution energy-dispersive gamma-ray spectrometer consisting of an array of 512 TES microcalorimeters divided into two arrays.[15,33] As the SLEDGEHAMMER array is similar to the proposed LXM x-ray microcalorimeter array, that is, the one we will review.

The SLEDGEHAMMER instrument has demonstrated readout of 128 microwave SQUID multiplexed channels on a single set of coaxial cables.[15] The readout noise was sufficiently low ($\sqrt{S_I} \approx 35\ \mathrm{pA}/\sqrt{\mathrm{Hz}}$) to not significantly degrade the energy resolution of the TESs (55 eV at 100 keV). A photograph of the fully assembled 256-TES sample box is shown in Fig. 3(a), with microwave signals entering and exiting the box through the subminiature version A (SMA) connectors in the four corners, passing through four 33-resonator multiplexing chips on either side, allowing for readout of the entire box on two pairs of coax. The resonator bandwidth of 300 kHz and spacing of 6 MHz for this demonstration were matched to the requirements of the slower gamma-rays sensors designed to operate at photon energies of up to 210 keV.

Although the SLEDGEHAMMER instrument is currently the largest array of TES microcalorimeters using microwave SQUID multiplexing, a similar multiplexing factor has been demonstrated on an array of 104 soft x-ray TESs. These sensors, with detector time constants of $\tau_{\mathrm{fall}} \approx 400\ \mu\mathrm{s}$ were integrated with microwave SQUID multiplexers as shown in Fig. 4(a), with the four microwave SQUID multiplexer chips at the outside of the box and the x-ray sensor array in the middle. The combined x-ray spectrum of 82 of the channels is shown in Fig. 4 for x-rays from the magnesium Kα line at 1.25 keV achieving an

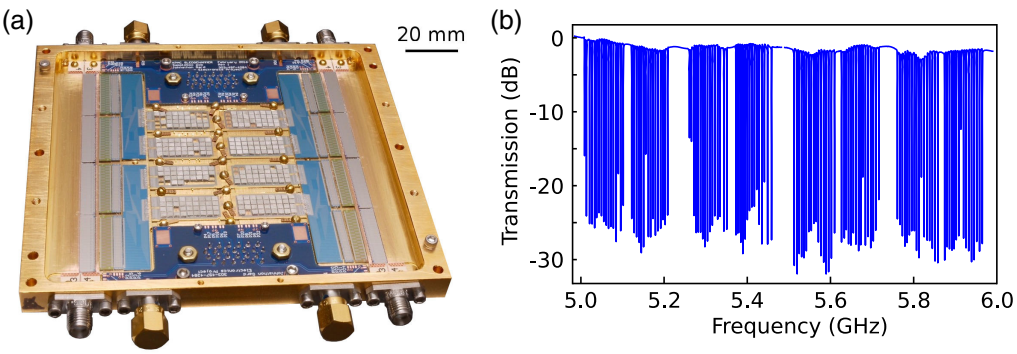

Fig. 3 (a) Photograph of the sample box containing 8 × 32-TES microcalorimeter detector chips (center), eight microwave multiplexer chips (outer vertical columns) and chips for detector bias, Nyquist filtering, and signal routing. Coax to microstrip to coplanar waveguide (CPW) adapters connect to the feedline on the multiplexing chips. (b) The microwave transmission through four microwave SQUID multiplexer chips on one side of the box showing resonance dips from 132 resonators.

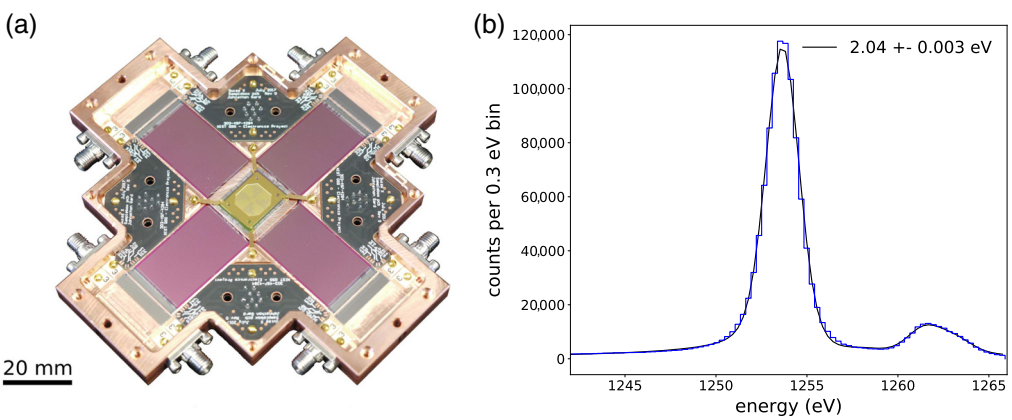

Fig. 4 (a) Photograph of the sample box for the 100 channel demonstration of microwave SQUID multiplexed readout of soft x-ray TESs. (b) Combined spectra from 82 TESs showing 2.04 eV resolution of the magnesium Kα line at 1.25 keV.

Downloaded From: https://www.spiedigitallibrary.org/journals/Journal-of-Astronomical-Telescopes,-Instruments,-and-Systems on 25 Apr 2019
Terms of Use: https://www.spiedigitallibrary.org/terms-of-use

energy resolution of 2.04 eV, consistent with the resolution achieved using TDM with the same array.

The same multiplexer designs were also used at NASA GSFC to read out an array of hard x-ray TESs.[34] The array had previously been measured with a conventional SQUID readout, nonmultiplexed, achieving a resolution of 2.8 eV FWHM at 5.9 keV. Five pixels from this array were multiplexed simultaneously achieving spectral resolutions between 2.8 and 3.1 eV FWHM.

The multiplexers used for these demonstrations do not have sufficient bandwidth to track the rising edge of pulses from the faster hydra microcalorimeters planned for the the LXM. However, microwave SQUID multiplexers with 2 MHz of bandwidth per resonator spaced by 14 MHz have also been demonstrated, see Fig. 5(a), although they are at an earlier state of development. These multiplexers have demonstrated appropriate modulation (~1.5 MHz), shown in Fig. 5(a), and readout noise of 20 pA/$\sqrt{\text{Hz}}$, shown in Fig. 5(b) and been measured at flux ramp rates as high as 800 kHz with $2\Phi_0$ ramp amplitude. These higher bandwidth designs have been used to measure high-speed x-ray TESs ($\tau_{\text{fall}} \approx 30\ \mu$s). Figure 6(b) shows a 1.35-keV pulse from magnesium Kα line at 1.25 keV. Figure 6(a) shows measured spectrum with a 1.37-eV FWHM resolution at 1.25 keV. Although these high-speed multiplexers have not yet been used in large scale demonstrations, they will soon be demonstrated in the HOLMES[35] and the TES x-ray spectrometer at second-generation Linac coherent light source (LCLS-II)[36] currently under development.

3 Optimizing Microwave SQUID Multiplexing for the LXM

In order to evaluate the suitability of microwave SQUID multiplexing for readout of the LXM arrays, we describe the fundamental readout noise and crosstalk levels that can be achieved and the process of optimizing the microwave SQUID multiplexers to match the LXM sensors. We then describe how these metrics were used to establish a baseline readout that meets the requirements of the LXM. Finally, we discuss the details of scaling the designs to meet the bandwidth requirements of the different LXM subarrays and progress toward demonstrating representative designs.

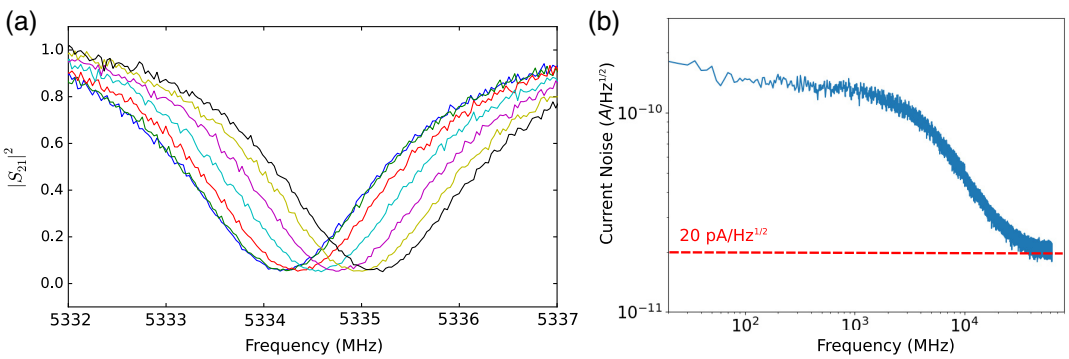

Fig. 5 (a) Measured $|S_{21}|^2$ as a function of frequency for seven different values of input current. The shifting of the resonance demonstrates the modulation range of the 2-MHz design. (b) Measured current noise spectral density from one channel of the microwave SQUID multiplexer with bandwidth of 2 MHz and the TES unbiased (i.e., in the superconducting state). The readout noise ($\sqrt{S_I} \approx 20$ pA/$\sqrt{\text{Hz}}$) can be seen above the roll-off of the TES noise.

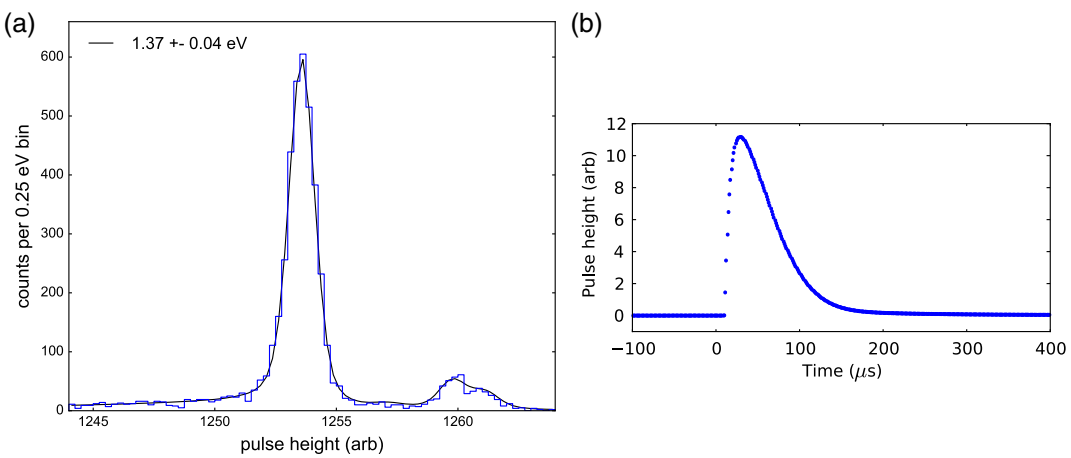

Fig. 6 (a) Measured spectrum showing 1.37 eV FWHM resolution of the magnesium Kα line at 1.25 keV measured at flux-ramp modulation at 800 kHz. (b) A fast x-ray pulse read out using microwave SQUID multiplexing and flux-ramp modulation at 800 kHz. Each sample represents the demodulation of one flux-ramp.

Downloaded From: https://www.spiedigitallibrary.org/journals/Journal-of-Astronomical-Telescopes,-Instruments,-and-Systems on 25 Apr 2019
Terms of Use: https://www.spiedigitallibrary.org/terms-of-use

3.1 *Fundamental Performance of Microwave SQUID Multiplexing*

The microwave SQUID multiplexer has two primary noise sources: HEMT amplifier noise and two-level-system (TLS) noise.[37] The TLS noise arises from the switching of two-level systems with electric dipole moments, coupled to the resonator. As these TLSs change state, they change the effective electrical length of the resonator, producing resonance-frequency noise. The power spectral density of this noise has characteristic $1/\sqrt{f}$ dependence on frequency. This dependence makes it the dominate signals close to the carrier. The HEMT is a broadband noise source and can be described by a noise temperature, typically $T_N \approx 3$ K. The HEMT noise dominates farther from the microwave carrier frequency because the TLS noise falls off with frequency. The frequency of modulation used is chosen to ensure the signal appears at a frequency where the TLS noise is subdominant.

The SQUIDs provide the gain that boosts both the signal and the noise of the detectors above the noise of the cryogenic HEMT amplifier. The effective gain is determined by two factors: the fractional change in the microwave transmission function and the power of the microwave tone probing the resonance. The optimal power per tone can be shown to be independent of the resonator bandwidth, so long as the frequency shift has been optimized to match, and is approximately −71 dBm. At this power level, we observe a readout noise level of 2 to 3 $\mu\Phi_0/\sqrt{\text{Hz}}$. With a typical input coupling of $M_{\text{in}} \approx 230$ pH,[15,33] this adds an input-referred current noise of 18 to 27 $\text{pA}/\sqrt{\text{Hz}}$. This noise is low enough not to degrade the TESs proposed for the LXM. If necessary, the current noise can be improved by increasing the input coupling, but the optimization of the noise needs to be balanced against other important sensor parameters such as dynamic range and crosstalk as will be discussed later in this section.

The SQUID response is linearized through the flux-ramp modulation[32] mentioned earlier. This is necessary because, while the response of an rf-SQUID to applied flux is periodic with a magnetic flux quantum Φ_0, this use of flux-ramp modulation provides a dynamic range that is effectively infinite, subject to a slew rate requirement. The flux-ramp demodulation algorithm, which must identify phase shifts of the SQUID response between one ramp period and the next, requires that the rapidly changing input signal during the rising edge of a pulse induce a change of less than half a flux quantum during a single flux ramp. Otherwise, it can for example confuse a phase shift slightly greater than π with a phase shift slightly less than $-\pi$. Close to this limit, it can also degrade signal-to-noise and introduce small systematic errors. For accurate flux-ramp demodulation, we therefore require the maximum input signal slew rate SR to obey

$$\text{SR} < \frac{\Phi_0 f_r}{2M_{\text{in}}}, \tag{1}$$

where f_r is the flux-ramp repetition frequency, typically 10 kHz to 1 MHz, and is also the effective sampling rate of the input signal.

A number of instruments under development plan to track the resonance frequency of each resonator using a feedback loop instead of using fixed frequency probe tones.[36,38] Since the probe tone spends more time deeper in the resonance less power per tone is transmitted to the amplifiers and mixers in the readout chain. This has the advantage of lowering the linearity requirements for the amplifiers and mixers. There is also potential to use this technique to ramp the resonator faster than specified in Eq. (1) and to get more than one demodulated phase data point per flux ramp. In this paper, we take a conservative approach and only consider techniques that have been previously demonstrated in TES microcalorimeters. Therefore, Eq. (1) will be used to define the maximum slew rate when considering configurations to meet the requirements of the LXM. However, any continuing advancements could be used to provide further margin.

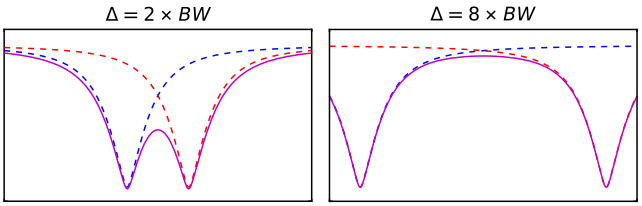

Fig. 7 Lorentzian transmission of a pair of resonators spaced at twice their bandwidth (left) and eight times their bandwidth.

Crosstalk requirements ultimately determine the frequency spacing between adjacent multiplexer channels. Due to the Lorentzian tails of each resonator's microwave transmission (Fig. 7), a change in frequency of one resonator leads to a change in measured transmission at its neighbors. It can be shown[11] that a change in one resonance frequency of $\Delta\omega$ leads to crosstalk into its neighboring resonators that in the worst case is $\frac{\Delta\omega}{16n^2}$, where n is number of bandwidths between resonators. Spacing resonators by ∼10 times their bandwidth thus leads to a maximum crosstalk below one part per thousand. Using the bandwidth set by input signal slew rate, this crosstalk constraint determines the number of resonances that can be packed in a block of readout bandwidth.

For a given application, there is a chain of optimizations: (1) a target current noise determines an input coupling, (2) a target slew rate determines a flux-ramp repetition rate, (3) the flux-ramp rate determines resonator bandwidth, and (4) a crosstalk requirement determines the spacing between resonances and therefore the number of channels that can be multiplexed on a single line.

For example, a resonator bandwidth of 2 MHz allows for a $2\Phi_0$ flux-ramp frequency of up to 500 kHz, satisfying the requirements [Eq. (1)] in which signals of interest have a peak slew rate of ∼2.3 A/s for an $M_{\text{in}} = 230$ pH. In general, the required bandwidth (BW) of each microwave SQUID resonator is

$$\text{BW} > \text{SR}\frac{4N_{\Phi_0}}{\Phi_0}\sqrt{\frac{S_\Phi}{S_{I(\text{target})}}}, \tag{2}$$

where N_{Φ_0} is the number of flux quanta swept out by each ramp and $\sqrt{S_\Phi}$ is the readout noise referred to magnetic flux, which for existing devices is on the order of 2 to 3 $\mu\Phi_0/\sqrt{\text{Hz}}$.[15]

3.2 *Microwave Multiplexing for the LXM Requirements*

Table 1 summarizes the proposed readout resulting from optimization to meet the LXM system requirements. This table estimates the number of HEMT amplifiers necessary to read out the

Downloaded From: https://www.spiedigitallibrary.org/journals/Journal-of-Astronomical-Telescopes,-Instruments,-and-Systems on 25 Apr 2019
Terms of Use: https://www.spiedigitallibrary.org/terms-of-use

pixel count of the various LXM subarrays, with a ~50% safety margin of resonator bandwidth relative to expected detector slew rate, and with the resonators spaced by seven times the bandwidth for low crosstalk.

The optimization of thermal multiplexing relative to electrical multiplexing is described elsewhere in this proceedings,[1] but results in a requirement of at most 16 HEMTs to be read out at once. As shown in Table 1, this requirement is satisfied, since the ultra-hi-res array will not be read out at the same time as the others.

Design parameters for the main array predict that the maximum slew rate during a pulse can be as high as 1.5 A/s for the fastest pixel. For an input coupling of $M_{\text{in}} \approx 170$ pH, this becomes $0.12\Phi_0/\mu$s, requiring a flux-ramp repetition rate of at least 250 kHz. To provide for this with a 50% margin, the proposed resonator bandwidth is 1.4 MHz spaced at 10 MHz, enabling readout of ~400 detectors (10,000 spatial pixels) on a single pair of coaxial cables and one HEMT. As described in Sec. 2.2, the National Institute of Standards and Technology (NIST) has designed and fabricated multiplexers that have 300 kHz and 2 MHz bandwidth resonators. Scaling parameters to make a 1.4-MHz bandwidth design for the main array is very low risk.

The LXM focal plane has been proposed to include two other subarrays. The enhanced main array covers a narrower field-of-view, but is intended to read out higher x-ray flux signals. This requires wider bandwidth per microwave multiplexer readout channel. The ultra-hi-res array uses non-hydra detectors to allow for 0.3-eV energy resolution at high count rates. This requires one microwave multiplexer channel per pixel, but at moderate bandwidth. The process of scaling microwave SQUID multiplexer designs to other bandwidths is described in the following section.

3.3 *Scaling the Bandwidth of Microwave SQUID Multiplexers*

The resonance width can be defined in terms of a dimensionless parameter known as the quality factor ($Q = \omega_0/\text{BW}$). The total Q of the resonator is determined by Q_i due to internal losses and Q_c due to the coupling between the resonator and the feedline as

$$\frac{1}{Q} = \frac{1}{Q_i} + \frac{1}{Q_c}. \tag{3}$$

If Q_c is significantly lower than Q_i, then Q_c determines the bandwidth of the resonance. For the quarter-wavelength CPW resonators, we routinely achieve Q_i values of 300,000, significantly higher than Q_c at all bandwidths required for the LXM.

An equation for Q_c is derived in Ref. 11 considering for a circulating energy in the CPW resonator of characteristic impedance Z_1, how much power leaks out through the coupling capacitor C_c onto the feedline Z_0. This yields

$$Q_c \equiv \frac{\omega_0}{\text{BW}} = \frac{\pi}{2|S_{13}|^2} = \frac{\pi}{2\omega_0^2 C_c^2 Z_0 Z_1}. \tag{4}$$

Increasing the bandwidth is therefore a simple matter of increasing the capacitance between the resonator and the feedline. It should also be noted that both Q_c and C_c must be different at different frequencies, to produce the same target bandwidth.

Across the 4 to 8 GHz bandwidth proposed for the LXM, the ideal coupling capacitor varies significantly. Therefore, the coupling is separately optimized for each sub-band. In practice, microwave simulation tools are used to simulate the coupling S_{13} through the coupling capacitor, with port 1 and port 2 being the two sides of the feedline and port 3 the resonator.

Once the bandwidth of the resonator is optimized, the frequency shift of the resonator must be matched to the bandwidth. If the peak-to-peak SQUID response is less than the bandwidth, then the multiplexer does not achieve optimum gain. If the peak-to-peak SQUID response is greater than the bandwidth, then there are sections of the flux ramp where the SQUID response is insensitive to input flux. Furthermore, if the peak-to-peak response is greater than the bandwidth, it becomes possible for the resonator to bifurcate, toggling between two self-consistent states of resonance frequency and internal energy.

The frequency of a quarter-wave resonator is shifted due to the screening of the termination inductance by the rf-SQUID, shown schematically in Fig. 8. An equation for this shift is also derived in Ref. 11. The change in frequency for small changes in load inductance is

$$\frac{\partial\omega}{\partial L} = -\frac{2\omega_0^2}{\pi Z_1}, \tag{5}$$

and the effective inductance presented by the rf-SQUID load, see Fig. 8, is

$$L(\Phi) = L_c - \frac{M_c^2}{L_S + L_J \sec[2\pi\Phi/\Phi_0)]}, \tag{6}$$

where L_c is the self inductance of the resonator termination, M_c is the mutual inductance between the SQUID and the resonator, L_s is the geometric self inductance of the SQUID, L_J is the Josephson inductance of the Josephson junction, and Φ is the flux in the SQUID. With the usual definition $\lambda = L_S/L_J$, we can write the peak-to-peak frequency shift as

$$\Delta\omega = \frac{2\omega_0^2}{\pi Z_1}\left(\frac{M_c^2}{L_s}\frac{2\lambda}{1-\lambda^2}\right). \tag{7}$$

To change the peak-to-peak frequency shift, we therefore tune M_c, again performing a separate optimization for each frequency band.

Using this strategy, we have optimized the microwave SQUID multiplexer for a variety of maximum input slew rates. Since the newest hydra prototypes have faster slew rates than the final versions, we designed for wider bandwidth than optimum for the enhanced main array. With both a 2-MHz design and an 8-MHz design in hand, we will be able to measure all prototype hydra microcalorimeters and demonstrate resonator bandwidth over the needed range.

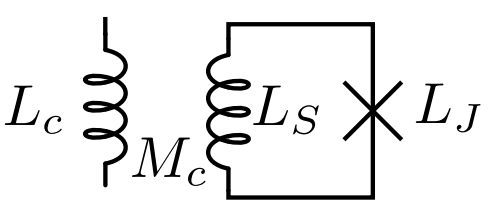

Fig. 8 Schematic of the inductor at the termination of the resonator L_c coupled to an rf-SQUID with inductance L_S with mutual inductance M_C. The rf-SQUID screens L_c and gives and effective inductance is a function of the input flux of the SQUID.

Downloaded From: https://www.spiedigitallibrary.org/journals/Journal-of-Astronomical-Telescopes,-Instruments,-and-Systems on 25 Apr 2019
Terms of Use: https://www.spiedigitallibrary.org/terms-of-use

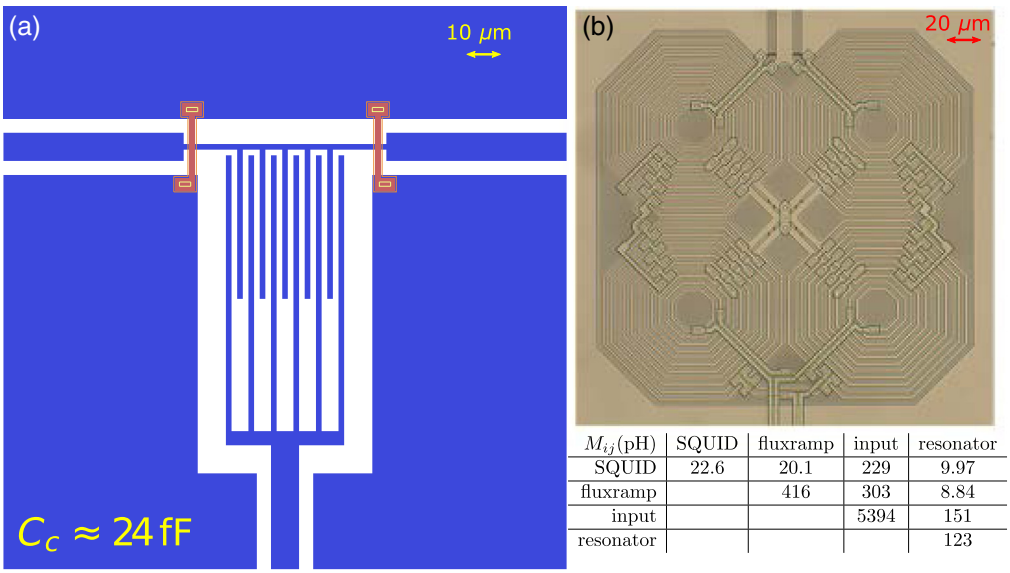

M_{ij}(pH)	SQUID	fluxramp	input	resonator
SQUID	22.6	20.1	229	9.97
fluxramp		416	303	8.84
input			5394	151
resonator				123

Fig. 9 (a) Example coupling capacitor between the resonator and the microwave feedline optimized for 8-MHz bandwidth. (b) Photograph of the gradiometric coupler between rf SQUID, resonator, input coupling coil, and flux-ramp coupling coil to optimize noise and slew rate for the LXM enhanced main array. The self inductances are on the main diagonal and the mutual inductances are on the off diagonal of the table.

The 8-MHz bandwidth design and fabrication are complete and the devices are currently being tested. The capacitive coupling to the resonator, shown in Fig. 9(a), was increased to $C_c \approx 24$ fF to achieve 8-MHz resonator bandwidth at 6 GHz. The coupling between the resonator and the SQUID was been increased to $M_c \approx 10$ pH, to match the 8-MHz bandwidth. The coupling was calculated using a three-dimensional inductance extraction program and the device is shown in Fig. 9(b).

3.4 *Advanced Spread Spectrum Multiplexers*

Microwave SQUID multiplexers have the potential for more efficient bandwidth utilization under low count rate conditions by the implementation of a spread-spectrum multiplexing (SSMux) design.[39] SSMux operates by combining circuit elements developed for microwave SQUID multiplexers and Walsh code-division SQUID multiplexers (CDM).[30] The SSMux takes the signal from each detector pixel and deliberately spreads it in the frequency domain across multiple microwave SQUID resonators to increase the multiplexing factor, see Fig. 10.

As previously described, the bandwidth required by each pixel in a microwave SQUID multiplexer is set by the maximum slew rate on the leading edge of the pulse. However, at any given time, few pixels are in the steep part of the leading edge of a pulse, where the slew rate is highest. The multiplexing factor and slew-rate budget can therefore be increased by spreading the flux signal from each pixel over N_{ss} resonators in a Walsh code. In SSMux, the signal from each TES is coupled to multiple resonators and each resonator is coupled to multiple TESs in a Walsh code. In this scheme, the total number of microwave SQUIDs is still equal to the number of pixels—which may be hydras—but the high slew rate of a pixel on the steep rising edge of a pulse is divided between N_{ss} different resonators, reducing the slew rate in each, and reducing the bandwidth each resonator requires. The reduction in required bandwidth makes it possible to pack the resonators closer, allowing a higher multiplexing factor in each HEMT, either reducing the number of HEMT channels, increasing the number of pixels, or expanding engineering margins (Fig. 10).

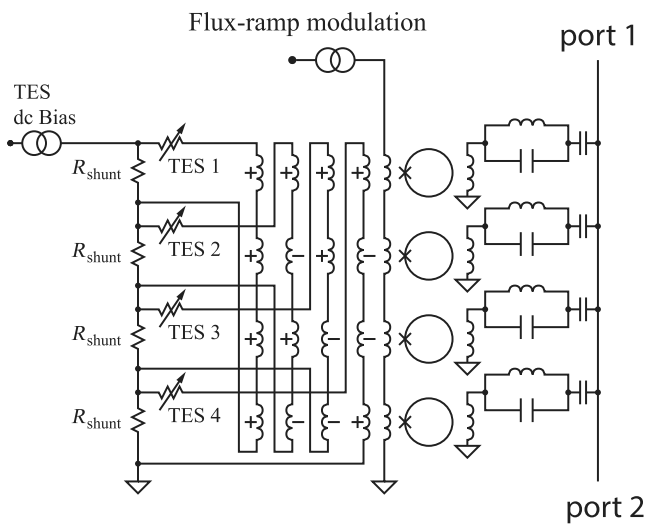

Fig. 10 The electrical schematic of a four-pixel implementation of spread-spectrum SQUID multiplexer (SSMux). The current from each TES couple to all four SQUIDs shown, with coupling polarities modulating in a Walsh code. There are an equal number of SQUIDs and TESs, but the flux-slew burden from the leading edge of an x-ray pulse is shared among all SQUIDs.

Walsh CDM of TES detectors into time-division multiplexed SQUIDs is well established.[30] With the N_{ss} detectors coupling to the N_{ss} SQUIDs according to an orthogonal Walsh code, the code can be inverted, extracting independent measurements of each TES. When the Walsh code is inverted, combining the N_{ss} measurements reduces the effective SQUID noise amplitude by $\sqrt{N_{ss}}$.

The mutual inductance M can therefore be reduced by as much as $\sqrt{N_{ss}}$. As long as only one of the TESs in the

Downloaded From: https://www.spiedigitallibrary.org/journals/Journal-of-Astronomical-Telescopes,-Instruments,-and-Systems on 25 Apr 2019
Terms of Use: https://www.spiedigitallibrary.org/terms-of-use

Walsh set is in a high-slew-rate condition at a given time, the maximum flux slew rate applied to this resonator is reduced by $\sqrt{N_{ss}}$, and the resonators can be spaced closer in frequency space, increasing the multiplexing factor by up to $\sqrt{N_{ss}}$. The analysis of this multiplex factor advantage is studied in detail in Ref. 39.

SSMux is both similar to and complementary to hydras. Hydras reduce the number of wires that must be extracted from the focal plane by implementing thermal multiplexing, but the scale of implemented hydras is constrained by pulse pileup. If an x-ray pulse arrives in one hydra subpixel during a pulse in another hydra subpixel, the energy resolution of both counts is significantly degraded. In contrast, SSMux does not reduce the number of leads extracted from the focal plane, but it scales more favorably with pulse pileup. An optimal implementation of an x-ray calorimeter system may incorporate both hydras and SSMux in a complementary configuration.

4 Discussion and Future Work

Microwave SQUID multiplexing has been demonstrated in a laboratory environment reading out 128 pixels on a single HEMT (limited by the bandwidth of the room-temperature electronics) and has been demonstrated reading out resonators with 2 MHz of bandwidth. The results of these demonstrations agree within a factor of 2 of the expected results. However, microwave SQUID multiplexing has yet to be demonstrated for hydra microcalorimeters. Therefore, with respect to the LXM requirements,[1] the current Technology Readiness Level (TRL) is TRL-3. To reach TRL-4, we will need to demonstrate microwave SQUID multiplexing of the LXM pixel types and achieve the expected performance, with respect to noise, slew rate, and crosstalk.

The NIST quantum devices group has been awarded funding through the NASA Astrophysics Research and Analysis Program (APRA) specifically to carry out this development in collaboration with the x-ray microcalorimeter group at NASA GSFC. The first step is to design and fabricate multiplexers appropriate for all the pixel types of the LXM. Simultaneously with the development of optimized designs, and perhaps as soon as early 2019, hydras provided by GSFC will be measured with microwave SQUID multiplexers to establish TRL-4. The milestones for achieving various TRLs are described in more detail in Ref. 1. We will then continue to optimize designs and perform the larger demonstrations on microcalorimeters representative of the LXM arrays achieving the necessary noise, slew rate, and channel spacing to establish TRL-5 in time to begin phase-A in 2024.

Acknowledgments

This work was funded by the NIST Innovations in Measurement Science Program and by the NASA Strategic Astrophysics Technology program. The authors have no relevant financial interests in the manuscript and no other potential conflicts of interest to disclose. This work was a contribution of a US government agency, not subject to copyright.

References

1. S. Bandler et al., "The Lynx x-ray microcalorimeter—LXM," *J. Astron. Telesc. Instrum. Syst.* (2019).
2. M. C. Weisskopf et al., "Chandra x-ray observatory (CXO): overview," *Proc. SPIE* **4012**, 2–16 (2000).
3. Lynx, "Lynx concept study (science)," wwwastro.msfc.nasa.gov/lynx/docs/science/ (2018).
4. Lynx, "Lynx concept study (instrument)," wwwastro.msfc.nasa.gov/lynx/docs/science/observatory.html (2018).
5. J. A. Gaskin, "The Lynx mission concept: 2017 accomplishments and 2018 goals," https://wwwastro.msfc.nasa.gov/lynx/docs/presentations/ (2018).
6. S. J. Smith et al., "Development of position-sensitive transition-edge sensor x-ray detectors," *IEEE Trans. Appl. Supercond.* **19**(3), 451–455 (2009).
7. K. D. Irwin and G. C. Hilton, "Transition-edge sensors," in *Cryogenic Particle Detection*, C. Enss, Ed., Springer, Berlin, Heidelberg, pp. 63–150 (2005).
8. J. N. Ullom and D. A. Bennett, "Review of superconducting transition-edge sensors for x-ray and gamma-ray spectroscopy," *Supercond. Sci. Technol.* **28**(8), 084003 (2015).
9. K. D. Irwin and K. W. Lehnert, "Microwave squid multiplexer," *Appl. Phys. Lett.* **85**(11), 2107–2109 (2004).
10. J. Mates et al., "Demonstration of a multiplexer of dissipationless superconducting quantum interference devices," *Appl. Phys. Lett.* **92**(2), 023514 (2008).
11. J. A. B. Mates, "The microwave SQUID multiplexer," PhD Thesis, University of Colorado (2011).
12. O. Noroozian et al., "High-resolution gamma-ray spectroscopy with a microwave-multiplexed transition-edge sensor array," *Appl. Phys. Lett.* **103**(20), 202602 (2013).
13. S. Kohjiro et al., "White noise of NB-based microwave superconducting quantum interference device multiplexers with NBN coplanar resonators for readout of transition edge sensors," *J. Appl. Phys.* **115**(22), 223902 (2014).
14. S. Kempf et al., "Multiplexed readout of MMC detector arrays using non-hysteretic RF-squids," *J. Low Temp. Phys.* **176**(3–4), 426–432 (2014).
15. J. Mates et al., "Simultaneous readout of 128 x-ray and gamma-ray transition-edge microcalorimeters using microwave squid multiplexing," *Appl. Phys. Lett.* **111**(6), 062601 (2017).
16. Y. Nakashima et al., "Readout of x-ray pulses from a single-pixel tes microcalorimeter with microwave multiplexer based on squids directly coupled to resonators," *J. Low Temp. Phys.* **193**, 618–625 (2018).
17. S. Kempf et al., "Design, fabrication and characterization of a 64 pixel metallic magnetic calorimeter array with integrated, on-chip microwave squid multiplexer," *Supercond. Sci. Technol.* **30**(6), 065002 (2017).
18. M. Wegner et al., "Microwave squid multiplexing of metallic magnetic calorimeters: status of multiplexer performance and room-temperature readout electronics development," *J. Low Temp. Phys.* **193**, 462–475 (2018).
19. T. Stevenson et al., "Magnetic calorimeter option for the Lynx x-ray microcalorimeter," *J. Astron. Telesc. Instrum. Syst.* **5**(2) (2019).
20. Lynx, "Lynx interim report," https://wwwastro.msfc.nasa.gov/lynx/docs/lynxinterimreport.pdf (2018).
21. S. Smith et al., "Multi-absorber transition-edge sensors for x-ray astronomy," *J. Astron. Telesc. Instrum. Syst.* **5**(2) (2019).
22. J. Chervenak et al., "Superconducting multiplexer for arrays of transition edge sensors," *Appl. Phys. Lett.* **74**(26), 4043–4045 (1999).
23. W. Doriese et al., "Developments in time-division multiplexing of x-ray transition-edge sensors," *J. Low Temp. Phys.* **184**(1–2), 389–395 (2016).
24. J. van der Kuur et al., "Multiplexed readout demonstration of a TES-based detector array in a resistance locked loop," *IEEE Trans. Appl. Supercond.* **25**, 1–4 (2015).
25. H. Akamatsu et al., "Development of frequency domain multiplexing for the x-ray integral field unit (X-IFU) on the Athena," *Proc. SPIE* **9905**, 99055S (2016).
26. R. Hijmering et al., "Readout of a 176 pixel FDM system for safari TES arrays," *Proc. SPIE* **9914**, 99141C (2016).
27. A. Bender et al., "Integrated performance of a frequency domain multiplexing readout in the SPT-3G receiver," *Proc. SPIE* **9914**, 99141D (2016).
28. B. Karasik and W. McGrath, "Novel multiplexing technique for detector and mixer arrays," *Proc. 12th Int. Symp. Space Terahertz Technol.*, San Diego, pp. 436–445 (2001).
29. G. Stiehl et al., "Code-division multiplexing for x-ray microcalorimeters," *Appl. Phys. Lett.* **100**(7), 072601 (2012).

Downloaded From: https://www.spiedigitallibrary.org/journals/Journal-of-Astronomical-Telescopes,-Instruments,-and-Systems on 25 Apr 2019
Terms of Use: https://www.spiedigitallibrary.org/terms-of-use

30. K. M. Morgan et al., "Code-division-multiplexed readout of large arrays of TES microcalorimeters," *Appl. Phys. Lett.* **109**(11), 112604 (2016).
31. P. K. Day et al., "A broadband superconducting detector suitable for use in large arrays," *Nature* **425**(6960), 817–821 (2003).
32. J. Mates et al., "Flux-ramp modulation for squid multiplexing," *J. Low Temp. Phys.* **167**(5–6), 707–712 (2012).
33. D. A. Bennett et al., "Integration of TES microcalorimeters with microwave squid multiplexed readout," *IEEE Trans. Appl. Supercond.* **25**(3), 1–5 (2015).
34. W. Yoon et al., "Toward large field-of-view high-resolution x-ray imaging spectrometers: microwave multiplexed readout of 28 TES microcalorimeters," *J. Low Temp. Phys.* **193**, 258–266 (2018).
35. B. Alpert et al., "Holmes," *Eur. Phys. J. C* **75**(3), 112 (2015).
36. D. Li et al., "TES x-ray spectrometer at SLAC LCLS-II," *J. Low Temp. Phys.* **193**, 1287–1297 (2018).
37. J. Gao et al., "Experimental evidence for a surface distribution of two-level systems in superconducting lithographed microwave resonators," *Appl. Phys. Lett.* **92**(15), 152505 (2008).
38. S. W. Henderson et al., "Highly-multiplexed microwave squid readout using the slac microresonator radio frequency (SMURF) electronics for future CMB and sub-millimeter surveys," *Proc. SPIE* **10708**, 1070819 (2018).
39. K. Irwin et al., "A spread-spectrum SQUID multiplexer," *J. Low Temp. Phys.* **193**, 476–484 (2018).

Biographies of the authors are not available.

Downloaded From: https://www.spiedigitallibrary.org/journals/Journal-of-Astronomical-Telescopes,-Instruments,-and-Systems on 25 Apr 2019
Terms of Use: https://www.spiedigitallibrary.org/terms-of-use